ChemPubSoc Europe

DOI: 10.1002/chem.201900587

CHEMISTRY
A European Journal
Communication

Nitrogen Heterocycles |*Hot Paper*|

[Co(TPP)]-Catalyzed Formation of Substituted Piperidines

Marianne Lankelma[+],[a] Astrid M. Olivares[+],[b] and Bas de Bruin*[a]

Dedicated to Professor Pablo Espinet on the occasion of his 70th birthday

Abstract: Radical cyclization via cobalt(III)-carbene radical intermediates is a powerful method for the synthesis of (hetero)cyclic structures. Building on the recently reported synthesis of five-membered N-heterocyclic pyrrolidines catalyzed by Co^{II} porphyrins, the [Co(TPP)]-catalyzed formation of useful six-membered N-heterocyclic piperidines directly from linear aldehydes is presented herein. The piperidines were obtained in overall high yields, with linear alkenes being formed as side products in small amounts. A DFT study was performed to gain a deeper mechanistic understanding of the cobalt(II)-porphyrin-catalyzed formation of pyrrolidines, piperidines, and linear alkenes. The calculations showed that the alkenes are unlikely to be formed through an expected 1,2-hydrogen-atom transfer to the carbene carbon. Instead, the calculations were consistent with a pathway involving benzyl-radical formation followed by radical-rebound ring closure to form the piperidines. Competitive 1,5-hydrogen-atom transfer from the β-position to the benzyl radical explained the formation of linear alkenes as side products.

Considerable efforts have been directed towards the synthesis of nitrogen-based heterocycles because of their importance in medicinal chemistry.[1] The most prevalent N-heterocycles in U.S. Food and Drug Administration approved drugs are piperidines (Figure 1).[2] Common synthetic routes to the piperidine motif include hydroamination and ring-closing metathesis.[3] Attractive alternative strategies for the formation of piperidines are ring-closing C–C bond forming reactions catalyzed by complexes based on earth-abundant transition metals.[4]

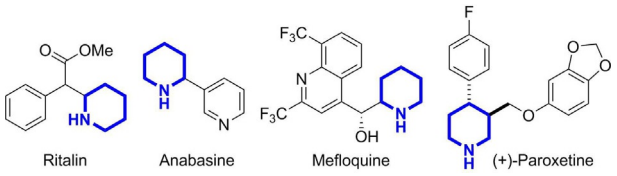

Figure 1. A few examples of piperidine-based drugs and natural products.

In recent years, our group and others have demonstrated that low-spin d^7 cobalt(II)-porphyrin complexes are excellent catalysts for C–C bond formation through radical-type carbene-transfer. In these reactions, the cobalt(II)-porphyrin reacts with a carbene precursor (usually a diazo compound or N-tosylhydrazone derivative) to form a Co^{III}-carbene radical, which can engage in controlled radical addition or hydrogen atom transfer (HAT). This type of reactivity belongs to a more general class of catalytic reactions involving single-electron elementary steps, called metalloradical catalysis.[5,21] Cobalt(III)-carbene radical chemistry has been successfully applied in the synthesis of carbo- and heterocyclic structures, including cyclopropanes,[6] chromenes,[7] furans,[8] indenes,[9] indolines,[10] ketenes,[11] butadienes and dihydronaphthalenes,[12] dibenzocyclooctenes,[13] as well as phenylindolizines.[14] Recently, the group of Zhang reported the synthesis of chiral pyrrolidines and related five-membered ring compounds, starting from N-tosylhydrazone derivatives and catalyzed by cobalt(II) complexes of D_2-symmetric chiral amidoporphyrins (Scheme 1 A).[15] Related reactions leading to five-membered N-heterocycles through carbene insertion into activated C–H bonds, mediated by Grubbs-type catalysts, were recently disclosed by the group of Fernández.[16]

As part of our ongoing exploration of the reactivity of cobalt(III)-carbene radicals and in view of the importance of six-membered N-heterocycles in medicinal chemistry, we sought to explore the feasibility of this approach for the development of a novel method to synthesize substituted piperidines (Scheme 1 B, compounds **2**). Furthermore, instead of starting directly from N-tosylhydrazones, we opted for the in situ formation of N-tosylhydrazones from aldehydes, followed by in situ deprotonation of the hydrazones to form the necessary diazo compounds. This one-pot approach reduces the number of synthetic steps and thereby provides accelerated access to the desired products. The potential of in situ formation of N-tosylhydrazone in other reactions was briefly illustrated in

[a] *M. Lankelma,[+] Prof. Dr. B. de Bruin*
Van't Hoff Institute for Molecular Sciences (HIMS)
Homogeneous, Supramolecular & Bio-Inspired Catalysis
University of Amsterdam, Science Park 904
1098 XH, Amsterdam (The Netherlands)
E-mail: b.debruin@uva.nl

[b] *A. M. Olivares[+]*
Department of Chemistry, University of Rochester
404 Hutchison Hall, Rochester, NY 14627-0216 (USA)

[+] *These authors contributed equally to this work.*

Supporting information and the ORCID identification number(s) for the author(s) of this article can be found under: https://doi.org/10.1002/chem.201900587.

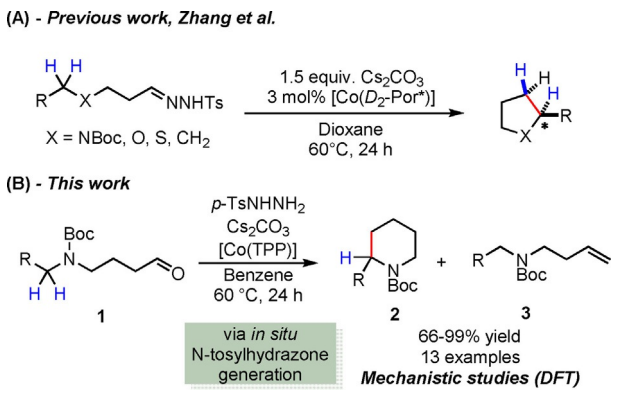

Scheme 1. (A) Formation of chiral pyrrolidines and other five-membered hetero- or carbocycles from N-tosylhydrazones, catalyzed by cobalt(II) complexes of D_2-symmetric chiral amidoporphyrins. (B) [Co(TPP)]-catalyzed one-pot synthesis of six-membered piperidine rings directly from linear aldehydes (this work).

2014 by the group of Che[17] and more recently by Chattopadhyay and co-workers.[14]

An initial screening proved this approach to be successful, yielding the targeted piperidines **2** in overall high yields. Linear alkenes **3** were obtained as side products, in most instances in small amounts (Scheme 1B). In this paper we describe the details of the catalytic reactions, including optimization studies, substrate screening, and mechanistic investigations aimed at understanding the formation of both ring products and linear alkenes.

The reaction parameters involved in the conversion of **1a** to **2a** and **3a** were screened in an effort to optimize product ratio and yield (Table 1; R = Ph). Without [Co(TPP)] (entry 0), only the diazo compound was formed. The use of 5 mol% [Co(TPP)], 1.2 equivalents of *p*-TsNHNH$_2$, 2 equivalents of Cs_2CO_3, benzene (1 or 2 mL) and 60 °C (entries 1 and 2) resulted in a quantitative combined yield and a **2a**/**3a** ratio of about 1:0.10. Increasing the catalyst loading (entry 3) did not have a beneficial influence on the product ratio. Addition of more than 1.2 equivalents of *p*-TsNHNH$_2$ (entry 4) or >2 equivalents Cs_2CO_3 (entry 5) was disadvantageous for both the yield and the product ratio.

Elevated temperatures (entries 6 and 7) promoted alkene formation, possibly due to an increased entropy contribution to $\Delta G^{\ddagger}$. Exclusion of light (entry 8) did not affect the yield or product ratio. The use of solvents that were less able to form π-stacking interactions compared with benzene (entries 9–11) did not improve the yield or product the ratio either, and in the case of toluene, the product ratio was even negatively affected. Notably, use of the isolated N-tosylhydrazone derivatives effectively provided the same results as the in situ generation from **1a**, however the latter approach allowed for faster access to the same products in the same yield and product ratio.

Next, we investigated the scope of the reaction (Table 2), applying the reaction conditions of entry 1 of Table 1. The reaction proved to be compatible with a wide variety of substituents (13 examples). We observed the relative amount of alkene to be dependent on the substitution of the substrate.

In most instances, piperidines **2** and alkenes **3** formed in a ratio varying between 1:0.07 and 1:0.28, but there seems to be a delicate balance between the product ratio and the stability of the proposed benzylic radical intermediate (see below). Steric bulk and/or considerable stability of this intermediate appears to induce substantial alkene formation (Table 2, entries c and d), whereas absence of radical-stabilizing substituents seems to favor ring closure. DFT calculations supported these observations (Schemes S4 and S16, Supporting Information).

Notably, in reactions leading to formation of five-membered N-heterocyclic pyrrolidines, no linear alkenes were formed as side products.[15] We wondered if this is due to a beneficial effect of the D_2-symmetric Co^{II}-amidoporphyrins used by Zhang and co-workers, or rather due to five-membered-ring formation being substantially more favorable than linear alkene formation. We therefore investigated the formation of pyrrolidine **4** using [Co(TPP)] and the above-described in situ approach (Scheme 2A). Interestingly, as in the report of Zhang and co-workers, this led to clean pyrrolidine formation without detectable amounts of linear alkene.

Table 1. Screening of conditions to optimize the yield and product ratio of the conversion of **1a** to **2a** and **3a**.

Entry	[Co(TPP)] [mmol]	*p*-TsNHNH$_2$ [mmol]	Cs_2CO_3 [mmol]	Solvent	Volume [mL]	Temperature [°C]	Yield	Piperidine:alkene ratio[d]
0[a,b]	0	0.12	0.20	benzene	2	60	0%	N/A
1[a]	0.005	0.12	0.20	benzene	2	60	quant.	1:0.10
2[a]	0.005	0.12	0.20	benzene	1	60	quant.	1:0.08
3[a]	0.015	0.12	0.20	benzene	2	60	quant.	1:0.14
4[a]	0.005	0.15	0.20	benzene	2	60	78%	1:0.40
5[a]	0.005	0.12	0.22	benzene	2	60	92%	1:0.42
6[a]	0.005	0.12	0.20	benzene	2	80	quant.	1:0.28
7[a]	0.005	0.12	0.20	toluene	2	105	96%	1:0.59
8[a,c]	0.005	0.12	0.20	benzene	1	60	quant.	1:0.07
9[a]	0.005	0.12	0.20	*o*-dichlorobenzene	2	60	85%	1:0.11
10[a]	0.005	0.12	0.20	toluene	2	60	quant.	1:0.51
11[a]	0.005	0.12	0.20	cyclohexane	2	60	85%	1:0.16

[a] 0.1 mmol substrate, 24 h. [b] Only the corresponding diazo compound formed. [c] Excluded from light. [d] Determined by integration of the ^{1}H NMR signals.

Table 2. Investigation of the substrate scope of [Co(TPP)]-catalyzed piperidine formation.

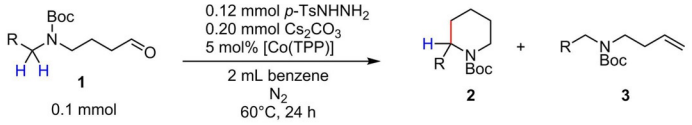

		Combined isolated yield (%)	Product 2 : 3			Combined isolated yield (%)	Product 2 : 3
a	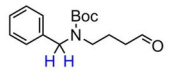	quant.	1 : 0.11	h	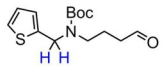	77%	1 : 0.07
b	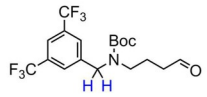	96%	1 : 0.23	i	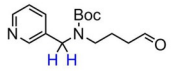	66%	1 : 0.10
c	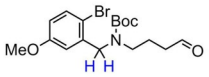	quant.	1 : 1.55	j	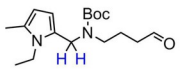	98%	1 : 0.07
d	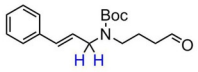	84%	*ca.* 1 : 1 [a]	k	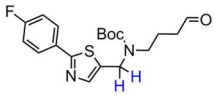	quant.	1 : 0.09
e	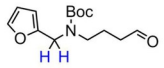	92%	1 : 0.16	l	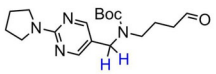	99%	1 : 0.19
f	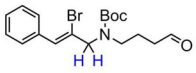	71%	1 : 0.22	m	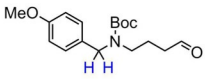	94%	1 : 0.08
g	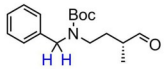	quant.	1 : 0.28				

[a] The overlap of the signals of **2d** and **3d** in ^{1}H NMR complicates proper determination of their ratio.

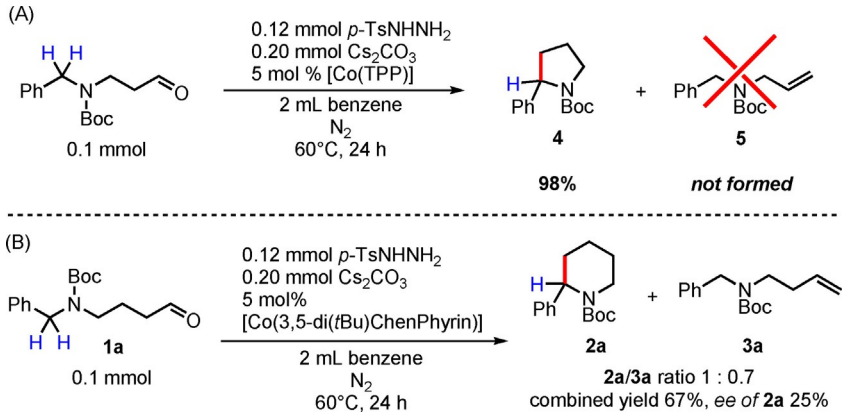

Scheme 2. (A) [Co(TPP)]-catalyzed formation of pyrrolidine **4** via in situ generation of the N-tosylhydrazone. (B) Formation of piperidine **2a** and alkene **3a** catalyzed by [Co(3,5-di(*t*Bu)ChenPhyrin)].

Furthermore, when using Zhang's D_2-symmetric chiral catalyst [Co(3,5-di(*t*Bu)ChenPhyrin)] to synthesize six-membered N-heterocyclic piperidine **2a** (Scheme 2B), we observed a larger amount of linear alkene than with [Co(TPP)]. With this catalyst, piperidine **2a** and alkene **3a** were formed in an almost equimolar ratio (1:0.70), which might be attributed to the formation of hydrogen bonds between the substrate and amide substituents of the porphyrin.[18] The products were obtained in poor combined yield (67%) compared with the [Co(TPP)]-catalyzed reaction, and asymmetric induction proved inefficient (*ee* of **2a**: 25%). Optimization of asymmetric induction with other chiral catalysts is beyond the scope of this Communication, but would be of interest for subsequent studies.

The above observations show that six-membered-ring formation and linear-alkene production are competitive, whereas linear alkenes are not formed in the synthesis of five-membered pyrrolidine rings, irrespective of the type of cobalt(II)-porphyrin used. Such behavior is not easy to understand in

terms of a mechanism involving linear-alkene formation through a commonly accepted 1,2-hydrogen shift (Scheme 3).[19]

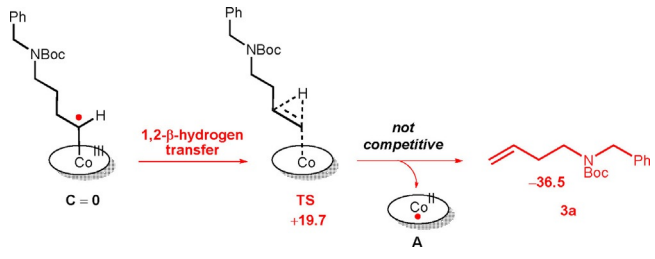

Scheme 3. Linear-alkene formation from cobalt(III)-carbene radical intermediate **C** by 1,2-HAT from the β- to the α-position has a rather high energy barrier. The ellipse represents the porphyrin ligand. All Gibbs free energies ($\Delta G^{\circ}_{333\,K}$, in kcal mol^{-1}) are reported relative to the energy of intermediate **C**.

To gain a better understanding of the mechanisms of cobalt(II)-porphyrin-catalyzed formation of pyrrolidines, piperidines, and alkenes, the reactions were investigated using DFT methods. To reduce computation time, a simplified porphyrin without phenyl substituents on the *meso*-positions, [Co(por)], was used . A first important observation is that alkene formation through the expected 1,2-HAT from the β-position to the carbene-radical carbon of the proposed intermediate **C** has a high computed free-energy barrier of +20 kcal mol^{-1} (Scheme 3). This barrier is too high to compete with radical-rebound ring closure to form **2a** (barrier: +7 kcal mol^{-1}; Scheme 4).

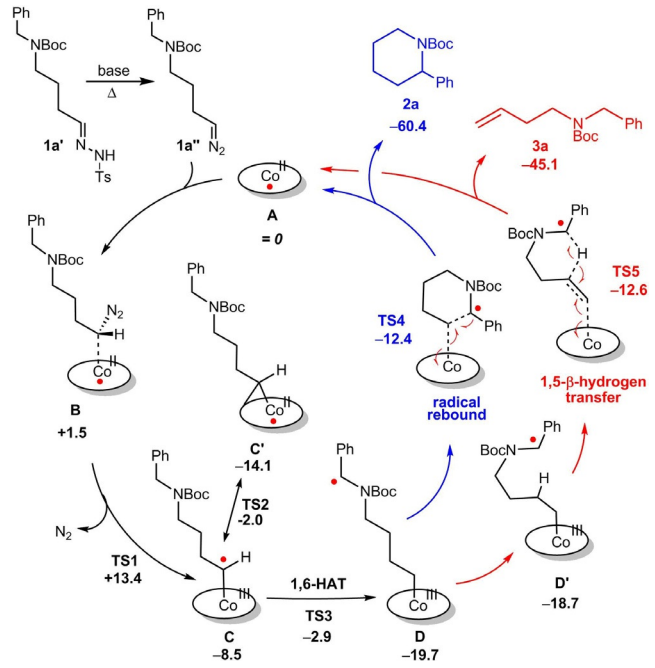

Scheme 4. Proposed mechanisms for [Co(por)]-catalyzed competitive formation of piperidines and alkenes. All Gibbs free energies ($\Delta G^{\circ}_{333\,K}$, in kcal mol^{-1}), including those of **TS1**–**TS5**, are reported relative to the energy of intermediate **A**. The ellipse represents the porphyrin ligand.

However, we found an alternative pathway for linear-alkene formation, involving 1,5-HAT from the β-position to the benzylic radical carbon of intermediate **D** over **TS5** (red pathway), which has a similar barrier as radical-rebound ring closure over **TS4** (blue pathway). As such, the DFT calculations point in the direction of the two competitive pathways depicted in Scheme 4.

The catalytic cycle is preceded by the (presumably) uncatalyzed formation of diazo compound **1a''** from N-tosylhydrazone **1a'** which is, in turn, in situ generated from aldehyde **1a**. Coordination of diazo compound **1a''** to the cobalt(II) porphyrin generates intermediate **B**. Dinitrogen loss from diazo adduct **B** over **TS1** to form cobalt(III)-carbene radical intermediate **C** is an exergonic, low-barrier process (+13.4 kcal mol^{-1}). Similar to previously reported cobalt(III)-carbene radical species, intermediate **C** carries most of its spin density localized at the carbene carbon.[20,21] An intramolecular 1,6-HAT process then relocates the radical center from the α-position to the ζ-position to yield benzyl radical intermediate **D** or its bent analogue **D'**. Intramolecular ring closure (effectively involving radical combination of the α- and ζ-positions) over **TS4** yields piperidine **2a**, whereas a 1,5-β-HAT over **TS5** leads to the formation of alkene **3a**. The almost identical **TS4** and **TS5** barriers suggest that these two pathways should be in close competition (see also Schemes S1, S3, and S15 in the Supporting Information). Although these DFT results explain the formation of both **2a** and **3a**, the computed barriers are too similar to explain the experimentally observed **2a**/**3a** ratio of 1:0.10. Therefore, we also explored alternative pathways involving six-coordinate intermediates.

The insertion of the carbene carbon of intermediate **C** into the bond between the metal and a pyrrolato nitrogen of the porphyrin can cause the carbene to adopt a bridging position (Scheme 4, **C'**).[21,22] A hexacoordinate species bearing both a bridging and a terminal carbene ($\mathbf{D}_{\mathbf{bridged}}$, Scheme S8, Supporting Information) could also be envisioned. When the pathways towards products **2a** and **3a** are computed starting from $\mathbf{D}_{\mathbf{bridged}}$ and passing through $\mathbf{TS4}_{\mathbf{bridged}}$ and $\mathbf{TS5}_{\mathbf{bridged}}$, the radical rebound and 1,5-β-HAT pathways remain too similar (see Schemes S8 and S20). For that reason, we also computed the energy barriers (from **D** onwards) for six-coordinated cobalt complexes formed upon coordination of a few different nitrogen-donor ligands at the axial position *trans* to the substrate. Ammonia, 1-methylimidazole, and pyridine were used as simplified computational models to study the effects of different axial ligands coordinated to cobalt under the applied reaction conditions.[23] Indeed, axial coordination to cobalt(III)-alkyl radical intermediate **D** changes the selectivity in favor of ring closure, and the different donors were found to have different degrees of influence on the product ratio (Schemes 5 and S9–S12).[24,25]

Coordination of ammonia resulted in a computed k_1/k_2 value of 10.4 (k_1 for piperidine formation, k_2 for alkene formation) at 60 °C, which is in accordance with the experimentally observed **2a**/**3a** ratio of 1:0.10.[26] The other axial donor ligands give rise to slightly different k_1/k_2 values (pyridine: 14.4; 1-methylimidazole: 5.9), suggesting that changes in the composition of the

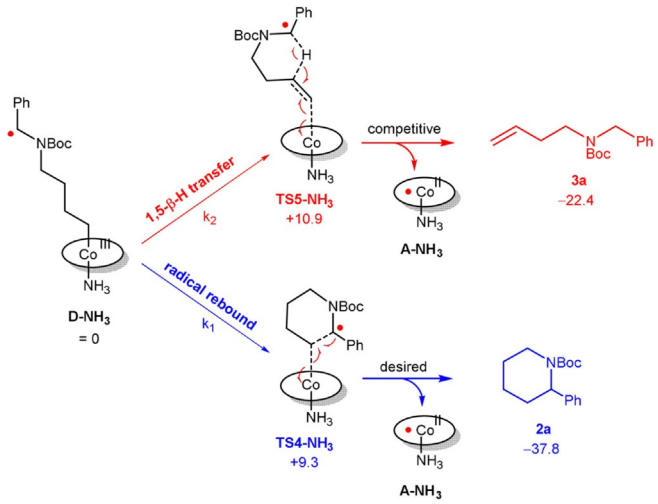

Scheme 5. The computed effect of coordination of NH_3 (as a simplified model for a variety of possible ligands)[23] on the energy barriers for [Co(por)]-catalyzed piperidine and alkene formation. All Gibbs free energies ($\Delta G^{\circ}_{333\,K}$, in kcal mol^{-1}), including those of **TS4** and **TS5**, are reported relative to the energy of intermediate **D-NH$_3$**. The ellipse represents the porphyrin ligand.

reaction mixture over time could indeed lead to a change in product ratio. This was experimentally confirmed, monitoring the reaction of **1a** by ^{1}H NMR spectroscopy over time indeed showed that the **2a**/**3a** ratio gradually shifts from 1:0.33 towards 1:0.10. We interpret this behavior as the result of a changing composition of the reaction mixture over the course of the reaction, with (on average) different axial ligands being coordinated to cobalt (see above).[23] The absolute amounts of piperidine and alkene formed over time clearly indicate that alkenes **3** are not converted to piperidines **2** (Figure 2, see Supporting Information for details).

To fully exclude the possibility that alkenes **3** could be converted to piperidines **2**, aldehyde **1a** was subjected to the general reaction conditions (Table 1, entry 1) in the presence of an equimolar amount of alkene **3h**. From all alkenes formed from the substrates listed in Table 2, **3h** was selected based on its ^{1}H NMR signature, which was most distinct from the ^{1}H NMR signatures of **2a** and **3a**. Based on ^{1}H NMR analysis, it was clear that no piperidine **2h** was formed from alkene **3h**; only

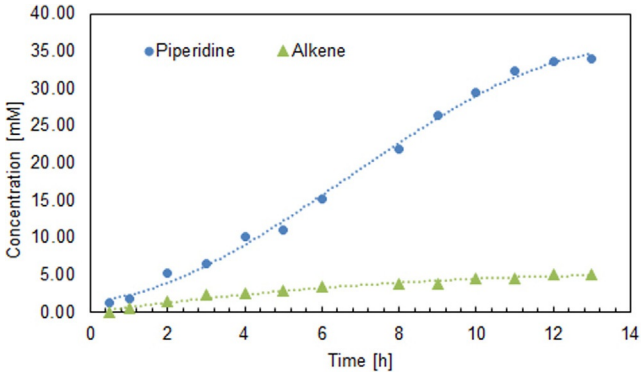

Figure 2. Monitoring piperidine and alkene formation over time.

piperidine **2a** as well as alkenes **3a** and **3h** were detected in the crude reaction mixture.

Lastly, we also computed the reaction pathway leading to five-membered pyrrolidines, in order to explain why the alkene formation is not in competition with this reaction. The results are detailed in the Supporting Information (Schemes S5–7 and S17–19) and are in excellent agreement with the experimental results. The DFT calculations confirm that [Co(por)]-catalyzed ring closure towards pyrrolidines has a much lower transition-state barrier than pathways leading to alkene formation. Neither alkene formation through 1,4-β-HAT nor through 1,2-β-HAT is competitive, with the computed barriers being, respectively, 8 and 11 kcal mol^{-1} higher in energy than the barrier for radical-rebound ring closure.

In conclusion, we developed a new base-metal-catalyzed synthetic route towards six-membered piperidine rings, which are important substructures of various medicinal compounds. Overall, the reaction is high yielding and compatible with a wide range of functional groups. In contrast to the cobalt(II)-porphyrin-catalyzed synthesis of five-membered pyrrolidines, the cobalt(II)porphyrin-catalyzed construction of piperidines is accompanied by formation of (generally small amounts of) olefinic side products. The relative amount of alkene was found to be dependent on the substitution of the substrate. DFT calculations indicate a mechanism involving 1,6-HAT from the carbene-radical carbon to the benzylic position of intermediate **C**, to form benzyl-radical intermediate **D**. The latter can undergo radical-rebound ring closure to form piperidines. A competitive 1,5-HAT from the β-position to the benzylic radical carbon explains the formation of linear alkenes as side products. DFT and ^{1}H NMR monitoring experiments suggest that an axial-ligand coordination influences the product ratio.

Acknowledgements

The work described in this paper was financially supported by the Netherlands Organization for Scientific Research (NWO TOP-Grant 716.015.001), the University of Amsterdam (Research Priority Area Sustainable Chemistry) and the National Science Foundation (Graduate Research Fellowship Program, NSF-NWO-GROW-project, no. DGE-1419118). We thank Prof. Dr. Joost N.H. Reek for a valuable suggestion, Ed Zuidinga for HRMS measurements and Dylan E. Parsons (University of Rochester) for helpful scientific discussions.

Conflict of interest

The authors declare no conflict of interest.

Keywords: C–C coupling · C–H activation · homogeneous catalysis · nitrogen heterocycles · radicals

[1] a) A. L. Mndzhoian, in *Synthesis of Heterocyclic Compounds*, Springer, **1959**; b) C. W. Bird, in *Comprehensive Heterocyclic Chemistry II*, Pergamon: Oxford, **1996**.

[2] a) E. Vitaku, D. T. Smith, J. T. Njardarson, *J. Med. Chem.* **2014**, *57*, 10257; b) R. D. Taylor, M. MacCoss, A. D. G. Lawson, *J. Med. Chem.* **2014**, *57*, 5845.

[3] a) I. Nakamura, Y. Tamamoto, *Chem. Rev.* **2004**, *104*, 2127; b) M. G. P. Buffat, *Tetrahedron* **2004**, *60*, 1701.

[4] a) *Earth Abundant Metals in Homogeneous Catalysis* (special issue): Guest Editors P. Chirik, R. Morris, *Acc. Chem. Res.* **2015**, *48*; b) *Non-Noble Metal Catalysis: Molecular Approaches and Reactions* (Eds.: R. J. M. Klein Gebbink, M.-E. Moret), Wiley **2019**, ISBN: 978-3-527-34061-3.

[5] Selected examples: a) A. Gansäuer, M. Behlendorf, D. von Laufenberg, A. Fleckhaus, C. Kube, D. V. Sadasivam, R. A. Flowers II, *Angew. Chem. Int. Ed.* **2012**, *51*, 4739; *Angew. Chem.* **2012**, *124*, 4819; b) A. Gansäuer, S. Hildebrandt, A. Michelmann, T. Dahmen, D. von Laufenberg, C. Kube, G. D. Fianu, R. A. Flowers II, *Angew. Chem. Int. Ed.* **2015**, *54*, 7003; *Angew. Chem.* **2015**, *127*, 7109; c) W. Hao, X. Wu, J. Z. Sun, J. C. Siu, S. N. MacMillan, S. Lin, *J. Am. Chem. Soc.* **2017**, *139*, 12141; d) P. F. Kuijpers, M. J. Tiekink, W. B. Breukelaar, D. L. J. Broere, N. P. van Leest, J. I. van der Vlugt, J. N. H. Reek, B. de Bruin, *Chem. Eur. J.* **2017**, *23*, 7945; e) H. Jiang, K. Lang, H. Lu, L. Wojtas, X. P. Zhang, *J. Am. Chem. Soc.* **2017**, *139*, 9164; f) V. Lyaskovskyy, A. I. O. Suarez, H. Lu, H. Jiang, X. P. Zhang, B. de Bruin, *J. Am. Chem. Soc.* **2011**, *133*, 12264; g) G. Manca, C. Mealli, D. M. Carminati, D. Intrieri, E. Gallo, *Eur. J. Inorg. Chem.* **2015**, 4885.

[6] a) L. Huang, Y. Chen, G. Y. Gao, X. P. Zhang, *J. Org. Chem.* **2003**, *68*, 8179; b) S. Zhu, J. V. Ruppel, H. Lu, L. Wojtas, X. P. Zhang, *J. Am. Chem. Soc.* **2008**, *130*, 5042; c) D. Intrieri, A. Caselli, E. Gallo, *Eur. J. Inorg. Chem.* **2011**, 5071; d) A. Chirila, B. G. Das, N. D. Paul, B. de Bruin, *ChemCatChem* **2017**, *9*, 1413; e) M. Goswami, B. de Bruin, W. I. Dzik, *Chem. Commun.* **2017**, *53*, 4382.

[7] a) N. D. Paul, S. Mandal, M. Otte, X. Cui, X. P. Zhang, B. de Bruin, *J. Am. Chem. Soc.* **2014**, *136*, 1090; b) N. Majumdar, N. D. Paul, S. Mandal, B. de Bruin, W. D. Wulff, *ACS Catal.* **2015**, *5*, 2329.

[8] X. Cui, X. Xu, L. Wojtas, M. M. Kim, X. P. Zhang, *J. Am. Chem. Soc.* **2012**, *134*, 19981.

[9] B. G. Das, A. Chirila, M. Tromp, J. N. H. Reek, B. de Bruin, *J. Am. Chem. Soc.* **2016**, *138*, 8968.

[10] a) A. S. Karns, M. Goswami, B. de Bruin, *Chem. Eur. J.* **2018**, *24*, 5253. For the synthesis of enantioselective indolines, see: b) X. Wen, Y. Wang, X. P. Zhang, *Chem. Sci.* **2018**, *9*, 5082.

[11] N. D. Paul, A. Chirila, H. Lu, X. P. Zhang, B. de Bruin, *Chem. Eur. J.* **2013**, *19*, 12953.

[12] C. te Grotenhuis, B. G. Das, P. F. Kuijpers, W. Hageman, M. Trouwborst, B. de Bruin, *Chem. Sci.* **2017**, *8*, 8221 – .

[13] C. te Grotenhuis, N. Heuvel, J. I. van der Vlugt, B. de Bruin, *Angew. Chem. Int. Ed.* **2018**, *57*, 140; *Angew. Chem.* **2018**, *130*, 146.

[14] S. Roy, S. K. Das, B. Chattopadhyay, *Angew. Chem. Int. Ed.* **2018**, *57*, 2238; *Angew. Chem.* **2018**, *130*, 2260.

[15] Y. Wang, X. Wen, X. Cui, X. P. Zhang, *J. Am. Chem. Soc.* **2018**, *140*, 4792.

[16] D. Solé, A. Amenta, M.-L. Bennasar, I. Fernández, *Chem. Commun.* **2019**, *55*, 1160.

[17] A. R. Reddy, C. Zhou, Z. Guo, J. Wei, C. Che, *Angew. Chem. Int. Ed.* **2014**, *53*, 14175; *Angew. Chem.* **2014**, *126*, 14399.

[18] Y. Wang, X. P. Zhang, "*[Co(3,5-Di-tBu-ChenPhyrin)]*" *e*-EROS, John Wiley & Sons, **2018**.

[19] a) M. P. Doyle, M. A. McKervey, T. Ye, *Modern Catalytic Methods for Organic Synthesis with Diazo Compounds*, Wiley-Interscience, New York, **1998**; b) G. Bertrand, *Carbene Chemistry*, Fontis Media, Lausanne, Switzerland, **2002**.

[20] a) H. Lu, W. I. Dzik, X. Xu, L. Wojtas, B. de Bruin, X. P. Zhang, *J. Am. Chem. Soc.* **2011**, *133*, 8518; b) W. I. Dzik, X. P. Zhang, B. de Bruin, *Inorg. Chem.* **2011**, *50*, 9896; c) W. I. Dzik, J. N. H. Reek, B. de Bruin, *Chem. Eur. J.* **2008**, *14*, 7594; d) V. Lyaskovskyy, B. de Bruin, *ACS Catal.* **2012**, *2*, 270.

[21] W. I. Dzik, X. Xu, X. P. Zhang, J. N. H. Reek, B. de Bruin, *J. Am. Chem. Soc.* **2010**, *132*, 10891.

[22] Involvement of a bis-carbene species was considered unlikely, based on previously published calculations. See reference [21].

[23] Under catalytic conditions the reaction medium changes, and various different donors could be coordinated to cobalt, not necessarily the same in the beginning and end of the reaction: for example, *p*-$TsNHNH_2$, the oxygen atoms of the base, the terminal nitrogen atom of the N-tosylhydrazone, the internal nitrogen atom of the deprotonated N-tosylhydrazone, and the terminal nitrogen atom of the diazo compound could all act as axial ligands.

[24] Only the relative energy barriers were significantly affected by these nitrogen-donor ligands. The absolute energy barriers remained similar.

[25] Effects of axial ligands coordinated *trans* with respect to the substrate have been extensively described before for metalloporphyrins. See for example, a) Y. Chen, X. P. Zhang, *Synthesis* **2006**, *10*, 1697; b) D. Balcells, C. Raynaud, R. H. Crabtree, O. Eisenstein, *Inorg. Chem.* **2008**, *47*, 10090; c) Y. Kang, H. Chen, Y. J. Jeong, W. Lai, E. H. Bae, S. Shaik, W. Nam, *Chem. Eur. J.* **2009**, *15*, 10039; d) S. P. de Visser, R. Latifi, L. Tahsini, W. Nam, *Chem. Asian J.* **2011**, *6*, 493.

[26] Note that these DFT calculations were performed in the gas phase and were simplified in several ways. Furthermore, the product ratio is calculated based on very small energy differences between the transition states of the k_1 and k_2 pathways, close to the accuracy of the calculations. The effects of axial-ligand coordination on the computed k_1/k_2 ratios should therefore not be over-interpreted.

Manuscript received: February 7, 2019

Accepted manuscript online: March 7, 2019

Version of record online: April 1, 2019

